

Characterization of gold nanoparticle layer deposited on gold electrode by various techniques for improved sensing abilities

Patricia Khashayar^{1,2,3}, Ghassem Amoabediny^{4,5}, Bagher Larijani⁶, Morteza Hosseini¹, Rik Verplancke², David Schaubroeck², Michel De Keersmaecker⁷, Annemie Adriaens⁷, Jan Vanfleteren^{2,*}

¹Nanobiotechnology Department, Faculty of New Sciences & Technologies, University of Tehran, Tehran, Iran

²Center for Microsystems Technology, imec and Ghent University, Gent-Zwijnaarde, Belgium

³Osteoporosis Research Center, Endocrinology and Metabolism Clinical Sciences Institute, Tehran University of Medical Sciences, Tehran, Iran

⁴Department of Biotechnology, Faculty of Chemical Engineering, School of Engineering, University of Tehran, Tehran, Iran

⁵Nanobiotechnology Department, Research Center for New Technology in Life Sciences Engineering, University of Tehran, Tehran, Iran

⁶Endocrinology and Metabolism Research Center, Endocrinology and Metabolism Clinical Sciences Institute, Tehran University of Medical Sciences, Tehran, Iran

⁷Department of Analytical Chemistry, Ghent University, Krijgslaan 281 (S12), Ghent, Belgium

*corresponding author e-mail address: jan.vanfleteren@elis.ugent.be

ABSTRACT

The deposition of gold nanoparticles (AuNPs) on the surface of gold electrode is believed to enhance the electrochemical characteristics of the surface. According to the existing literature, this could be performed in various ways. The purpose of the current study was to compare these results and report the most effective technique. In this regard, the layer-by-layer deposition, self-assembled monolayer technique and electro deposition method were investigated. Our results showed that cyclic voltammetry electrodeposition of AuNPs causes an observable increase in the peak current, causing improved electrode kinetics and a reduction in the oxidation potential (thermodynamically feasible reaction). These modified electrodes also showed several advantages with respect to stability and reproducibility.

Keywords: *Voltammetry; Gold Nanoparticles; Gold Electrode; Electrodeposition.*

1. INTRODUCTION

Over the past decade, more and more research has been performed on the use of nano-sized metal particles, particularly noble metal nanoparticles with controlled size, morphology, and crystal orientation, as their physical and chemical properties differ from that of the bulk material [1, 2]. These noble metal nanoparticles are becoming more popular in electrochemical sensing devices, as many studies have suggested that the use of modified electrodes can improve the performance of an electrochemical sensor [3].

Among the noble metal nanoparticles, gold nanoparticles (AuNPs) are of particular interest not only because of their stability, but also because of their specific physicochemical properties, including the enhanced diffusion of electroactive species based on their high effective surface area, improved selectivity, catalytic activity, and higher signal-to-noise ratio and conductivity [4, 5]. Important here, AuNPs provide a stable surface for enzyme immobilization and overcome the need for external electron-transfer mediators in electrochemical sensing [6].

In this regard, much attention has been focused on the analytical applicability of electrodes covered with AuNPs. Diverse strategies have been reported to coat various working electrodes such as platinum, carbon and gold with a layer of AuNPs [7, 8].

These coating techniques include layer-by-layer (LBL) deposition of AuNPs, self-assembled monolayer (SAM) development, sol-gel technique, impregnation, co-precipitation, metal organic-chemical vapor deposition, incipient wetness, electrodeposition and dip-coating [9, 10]. Some of them, such as the fabrication of metal nanoparticle layers using electron-beam lithography (EBL) or nanotemplating, require expensive equipment or special templates and are thus less commonly used [11]. Many studies have also reported that the use of electrodeposition techniques is preferred, compared to physical vapor deposition (PVD) methods, because of their relatively low-cost, and potentially higher deposition rate and film thickness [12, 13].

The results of these reports provide us with standard procedures for preparing Au nanocrystallites of controlled size and density with acceptable stability for biosensing purposes. In this work, we compare the most common existing methods for depositing gold nanoparticles on gold electrodes for electrochemical sensing purposes and present an optimized, adopted protocol to increase the surface area and analytical performance. A thorough evaluation of the optimum method is also provided.

2. EXPERIMENTAL SECTION

2.1. Chemicals and Materials.

All solutions were prepared using deionized water and chemicals of analytical grade were used as received without

further purification. Gold (III) chloride trihydrate (HAuCl₄), trisodium citrate dihydrate (≥99%), 1, 8-octanedithiol, poly (diallyldimethylammonium chloride) solution (PDDA, Mw 100

000 ~ 200 000), L-Glutathione reduced (GSH), and potassium hexacyanoferrate (III) ($K_3Fe(CN)_6$) were purchased from Sigma-Aldrich.

2.2. Instruments and Measurements.

All electrochemical experiments were performed using a computer-controlled Autolab PGSTAT101 (Metrohm, The Netherlands). They were carried out in a solution container, at room temperature (23 °C), using the three-electrode configuration fabricated in our laboratory according to the procedure described in this article. Electroactive substance 0.1 mM $K_3[Fe(CN)_6]$ and 0.5M H_2SO_4 were used as electrolyte solutions to verify whether the electrodes were modified with AuNPs in each approach.

Electrode surface topography as well as the morphology of the Au deposits were measured using Sirion field emission gun scanning electron microscopy (FEG-SEM) (FEI Nova 600 Nanolab Dual-Beam FIB) and atomic force microscopy (AFM). Most high resolution FEG-SEM pictures with magnifications $>2.5kx$ were achieved in "immersion mode" and with the TLD-SE detector (Through the Lens Detector). AFM images were acquired on a XE-70 (Park Systems) in non-contact mode ($15 \times 15 \mu m^2$) using Nanosensors tm (PPP-NCHR). The UV-Vis measurements were carried out on a UV Visible Spectrophotometer SPECORD 250 (Analytik Jena, Germany).

Scanning transmission electron microscopy (STEM), (Jeol Zeiss - EM10C JEM-2200FS FEG (S) TEM)- 80operated under high tension of 200 kV), was used to collect information for the visualization of the prepared gold nanoparticles. The samples were prepared using a gold (Au) TEM grid purchased from TED PELLA, INC (Sweden). A high angle annular dark field (HAADF) detector was used to distinguish the smallest and dispersed prepared gold nanoparticles from the porous gold substrate. A bright field detector (BF) was used to visualize larger prepared nanoparticles. The transmission electron microscopy (TEM) images were obtained with an EM10C 80 KV (Zeiss, Germany) transmission electron microscope. The zeta potential was measured by dynamic light scattering (DLS) (MALVERN Instrument MAL1001767 UK), at a temperature of 25 °C and a pH of 7.4.

2.3. Preparation of Gold Nanoparticles.

A modified Turkevich and Frens method was applied [14]. In this regard, 200 ml of 0.01 % $HAuCl_4$ solution was heated with gentle stirring. As soon as the solution was boiling, 4.5 ml of 1 % trisodium citrate dehydrate was rapidly added and boiling was pursued for an additional 15 min. The solution was stirred continuously after removing the beaker from the hot plate until the color of the solution turned brilliant red. This solution was stored at 4°C for further use. The characteristics and size of the developed AuNPs were checked using UV-Vis spectroscopy, TEM analysis and zeta potential measurements.

2.4. Preparation of PDDA-Protected AuNPs.

Hereof 250 μ L of PDDA solution, 40 mL water, 200 μ L 0.5M NaOH and 100 μ L $HAuCl_4$ (10mg/mL) were mixed and subsequently heated to 100°C with gentle stirring until the color changed to red [15].

2.5. Preparation of GSH-modified AuNPs.

A stock solution of glutathione (10mM) was prepared. Dilute HCl solution (10mM, 100 μ L) was added to gold aqueous solution (3 mL) to lower the pH (~4) [16]. An aliquot of GSH solution (10mM, 30 μ L) was added to the acidic gold aqueous solution, until the color changed from deep red to blue, indicating formation of aggregates amongst AuNPs.

2.6. Preparation of Gold Electrodes.

White float glass substrates were thoroughly cleaned to remove organic residues. They were firstly soaked in RBS aqueous detergents, which assure wetting and penetrating actions on the residues. The mechanical effect of an ultrasonic bath then permitted the removal and dispersion of the residues. The cleaned substrates were finally rinsed by soaking in isopropanol and DI water, and dried. Next, a 50 nm thick titanium tungsten (TiW (10%/90%)) adhesion enhancement layer and a 100 nm thick gold film were sputter deposited within one vacuum cycle of an Alcatel SCM600 system. Both metal films were subsequently patterned by photolithography and subsequent wet etching. To this end, positive photoresist S1818 was used as masking layer to wet etch both metal films. A 1.8 μ m thick coating of S1818 was spin-coated at 4000 rpm for 60 s and soft baked on a hot plate for 2 min at 90 °C. Next, the photoresist was UV exposed through a mask with the desired pattern for 7.5 s at 13 mW cm^{-2} , developed for 30 s in 50 % Microposit™ developer and hard baked for 30 min in a convection oven at 120 °C. The gold and titanium tungsten films were then wet etched using a solution of iodine (I_2) and potassium iodide (KI) (1:4 (1g I_2 , 4g KI, 73ml H_2O)) at room temperature, and a 30 % H_2O_2 solution at 55 °C, respectively. Finally, acetone was used to strip the remaining photoresist from the electrode surface.

Since the connection lines between the electrodes and their connections points were all made of gold, SU-8 was used as an insulation layer to cover the whole surface, exposing just the electrodes to the electrolyte solutions (Figure 1). In this regard, TI PRIME was first spin-coated on the substrate to improve the adhesion of SU-8 to the glass substrate. A 10- μ m thick layer of the negative-tone photoresist SU-8 3010 was then spin-coated on the substrate. After the soft bake (65°C for 1 min, followed by 95°C for 3 min), the substrate was allowed to cool down to room temperature. Next, the coating was exposed to UV radiation (300 mJ/cm^2) through a glass mask, using a double side mask aligner (EVG 620; Austria). A long pass filter was used to eliminate UV radiation below 350 nm. After the post-exposure bake (65°C for 1 min, followed by 95°C for 2 min), the SU-8wasdeveloped (90s in SU-8 developer), followed by a rinse in IPA. Finally, a hard bake was performed (120°C for 90 min) to further cross-link the SU-8, after which the substrates were diced.



a)

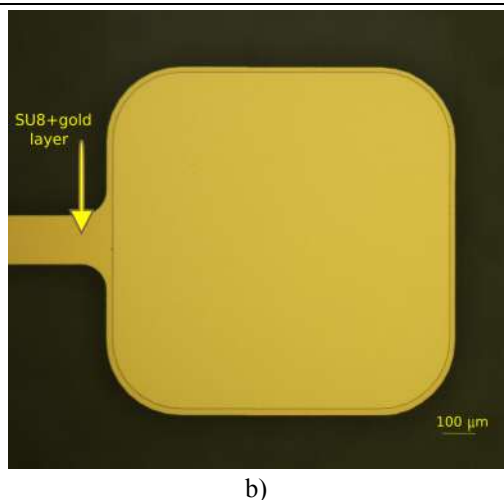


Figure 1. a) Schematic illustration of the cross-section of an electrochemical chip b) Optical microscope image of one of the electrodes on the electrochemical chip with SU-8 layer on its edges and connection line

2.7. Cleaning of Gold Electrodes.

Cleaning was performed using electrochemical pretreatment by cycling the electrode from large positive to negative potentials in sulfuric acid multiple times. The peak-current potential-differences obtained from cyclic voltammetry were used to compare the cleanliness of the gold electrodes. In this regard, the gold electrodes are cycled in 50 mM H_2SO_4 solution from -0.4 V to +1.4V, at 100 mV/s scan rate, until a stable cyclic voltammogram (CV) was achieved [17].

2.8. Surface Modification of Gold Electrodes with Gold Nanoparticles.

Deposition of the gold nanostructures was performed through different methods. Some of them are simple modifications of methods adopted from literature, whereas others are replications of techniques previously used for other purposes.

Method 1: Layer-by-layer deposition of AuNP

a) Multilayer AuNP-electrodes were fabricated by depositing 2 μl of a prepared aqueous solution of AuNP on the gold electrodes, which was subsequently dried at room temperature. This process was repeated three times. The electrodes were rinsed with deionized water and dried in a stream of nitrogen gas before the next layer deposition.

b) In order to improve the results, the layer-by-layer (LBL) deposition technique was applied [18]. The LBL method is based on the alternate deposition of oppositely charged (bio-) polymers, in our case PDDA [19]. The same process as mentioned in method 1a was repeated using PDDA-protected AuNPs. The electrode was rinsed with deionized water and dried in a stream of nitrogen gas before the next layer deposition.

3. RESULTS SECTION

The use of AuNP-coated gold electrodes has gained increased attention, particularly in electrochemical biosensing applications [26]. This is contributed to the fact that these

c) According to another method in literature, the previous process was repeated on a GSH-modified gold electrode [20].

d) The gold electrode was immersed in PDDA solution (20% aq. solution in 0.5M NaCl) for 10 to 30 min. After drying, 2 μl of prepared aqueous solution of GSH-modified AuNP was deposited on the gold electrode and dried at room temperature [21]. This process was repeated three times. The electrode was rinsed with deionized water and dried in a stream of nitrogen gas before the next layer deposition.

e) In another attempt, the PDDA-coated substrate was immersed into HAuCl_4 solution (10mg/mL) for 15 min [22]. Thereafter, the electrode was rinsed with deionized water and dried under N_2 before the next layer deposition. Subsequently, the electrode was placed in 0.1M KNO_3 solution, and -0.4V potential was applied for 60s. The process was repeated three times.

Method 2: Self assembled monolayer (SAM) development.

A SAM was prepared by immersing gold electrodes into 1mM 1, 8-octanedithiol in ethanol for 24 h in a dark environment at room temperature [23]. The modified electrodes were then taken out, soaked in distilled water and subsequently dried in a stream of nitrogen gas.

Method 3: Electrodeposition.

Electrodeposition was performed in an aqueous solution of 1.0mM HAuCl_4 and 0.5M H_2SO_4 in the presence of 0.1mM NaCl as the supporting electrolyte. Various protocols were applied.

a) Cyclic voltammetry: Electrodeposition was performed by CV scanning the potential from -0.5 V to +0.5 V, +1.0 V and 1.5 V at a scan rate 0.1 V/s for a given number of scans [24]. The process was repeated until the CV became reproducibly stable. The sweeping potential, the scan rate and the number of cycles needed were then optimized based on the results. This method is called 'ECV' all throughout this article.

b) Pulsed electrodeposition: The potential was stepped from -0.5V to +0.5 V, +1.0 V and +1.5V with a 5s deposition time [25].

2.9. Reproducibility, reusability, and stability of the electrodes.

The reproducibility of the electrodes was tested by comparing the cyclic voltammograms of electrodes prepared using each technique. Electrodes with less than 5% difference in the peak current were considered reproducible. The reusability of the electrodes prepared using each of the abovementioned methods was assessed through evaluating current change during 10 successive CV cycles. The stability of the immobilization process was also studied by continuously stirring the electrodes in water during 20 min. This process was repeated four times. As for the storage stability, the cyclic voltammograms of the electrodes preserved at room temperature for a week were compared with that of a freshly prepared electrode using the same method.

electrodes enhance the analytical performance of the sensor through providing a suitable microenvironment for biomolecule immobilization, their effects on increasing the surface area of the

exposed gold and facilitated electron transfer between the immobilized proteins and electrode surfaces. According to the existing studies, AuNP deposition results in three-dimensional Au deposits, which have a higher desire to adsorb specific functional groups [27, 28]. The size, structure, and distribution of these structures, however, have a strong effect on the performance of the system and thus should be well controlled.

As mentioned earlier some of the most common techniques reported in the literature are to be compared in this article to determine an optimized adopted protocol for depositing gold nanoparticles on gold electrodes with the aim of improving the performance in electrochemical biosensing purposes. In the following, the pros and cons of the methods described in the material and method section are described.

3.1. Gold nanoparticle deposition techniques.

Method 1:

Previous studies have suggested that the interactions in the spherical electron density around the gold atoms are responsible for the gold-gold bond in a reliable way [29]. Moreover, some studies have shown the high binding affinity of the terminal functional groups on the periphery of the ligand shell of the gold nanoparticles and the gold electrode surface [30]. They have shown the occurrence of the ligand replacement reactions when this binding affinity exceeds that of the ligand to the particle. As a result, we checked the affinity of our citrate-capped gold nanoparticles toward the gold electrode in method 1a. First the characteristics of the prepared gold nanoparticles were assessed in order to eliminate any chance of aggregation between the particles.

a) Density and size characterization of the prepared gold nanoparticles: First, the size and size-distribution of gold nanoparticles developed using the Turkevich and Frens method is reported to be dependent on the concentrations of gold salt, trisodium citrate, temperature and mixing rate [31]. The size of the gold nanoparticles developed in our study was determined by measuring the diameter of whole particles on TEM images. The diameter of gold nanoparticles from the highly monodisperse aqueous gold solution used in the present study was in the range of 5-10nm with very few particles of higher and lower size distribution (Figure 2). These images also showed that most of the gold nanoparticles are spherical in shape.

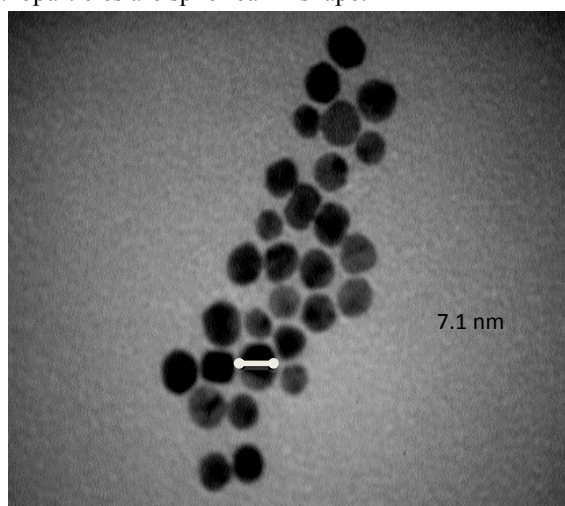


Figure 2. TEM images of monodisperse AuNPs.

The hydrodynamic diameter of nanoparticles was measured using azeta-sizer nano-ZS (Figure 3). The peak mean, about 7.5 nm, shows the mean diameter of the majority of the particles according to intensity. The particles had a mean zeta potential of 97 mV.

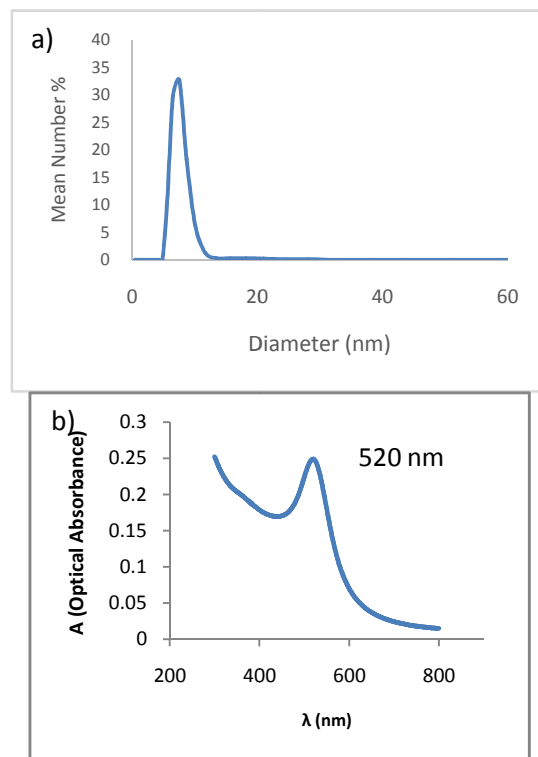


Figure 3. a) Size distribution of nanoparticles based on DLS results b) Absorption spectra of the AuNP aqueous solution.

UV-Vis Spectrophotometry is another important tool in determining the characteristics of gold nanoparticles. The width of the absorption spectra is related to the size distribution range of the nanoparticles and with increasing particle size, the absorption peak shifts to longer wavelengths. Generally, gold nanospheres display a single absorption peak in the visible range between 510-550 nm, mainly at 520 nm due to gold's surface plasmon resonance properties. In the present study, similarly, the UV-Vis spectrum showed only one band with a maximum λ at 520 nm (Figure 2). The lack of a band at around $\lambda=680$ nm indicates the absence of aggregated gold particles [32]. As for the PDDA-protected AuNPs, the band was shifted rightward to $\lambda_{max}=523$ nm.

b) Analysis of the AuNP layer on gold electrode: The results of the CV analysis showed that adding a layer of AuNP using method 1a did not affect the results significantly (Figure 4). While adding an AuNP-layer is believed to provide a larger surface area for the subsequent layers to bind, the unstable attachment between AuNPs and the electrode might be the reason behind the absence of any change in the results. Similar, results were noted for electrodes modified using method 1c.

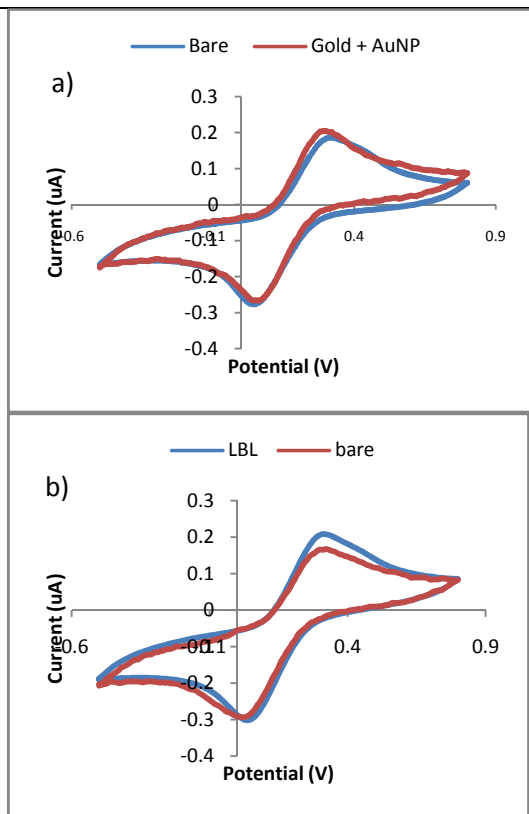


Figure 4. Comparison of voltammograms of bare electrodes and electrodes developed by a) method 1a and bare and b) method 1b and bare in 0.1 mM $K_3[Fe(CN)_6]$.

PDDA (also known as glue) is commonly used as a reducing and stabilizing agent to avoid AuNP aggregation. As it can be deposited by LBL, the water-soluble, quaternary ammonium, cationic polyelectrolyte enables control over the total AuNP/polymer thickness. The negatively charged substrate also improves attachment of positive compounds.

While our results showed the stronger attachment of PDDA-protected AuNPs to the underlying layers, their non-conductive nature was unfavorable in biosensing processes. This was shown based on a slight decrease in peak current, suggestive of reduced conductivity of the surface, in CV results (Figure 4). On the other hand, adding PDDA to the process did not improve the bonding of gold nanoparticles to the electrode surface significantly and thus no significant improvement was noted in the stability results (more than 5% variability in peak currents of 10 successive CVs). Similar results were noted after surface modification using methods 1d and 1e.

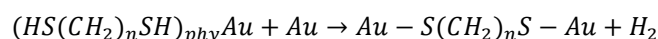
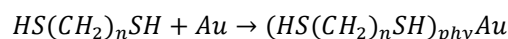
Method 2:

SAM could be achieved after deposition of cysteamine, mercaptocarboxylic acid, 3,3'-dithiodipropionic acid, 2-mercaptoethanesulfonate, 4-aminothiophenol, triazole and ultra fine polypropylene tetradecyl sulfate as well as by the composite 11-mercaptopundecanoic acid – polyethylene glycol and many other options on gold electrodes [33, 34]. It has been proven that the three-dimensional monolayers of S-containing organic compounds facilitate the electron transfer in the redox reaction occurring at the electrode-solution interface, ensuring an easier access of reagents to the electrode surface [35].

A thiol molecule consists of (1) a sulfur head group, which forms a strong, covalent bond with the gold electrode, (2) a hydrocarbon chain of variable length, which stabilizes the SAM

through van der Waals interactions, and (3) a terminal group, which has different functionalities. In our case, the –SH-terminated thiols of the dithiol used made the binding of metallic ions of the gold electrode and gold nanoparticles to the SAM possible [36]. Studies have shown that the adsorption time depends on the nature of the molecule, adding that dithiol deposition from solution needs less time [37]. This is while long chain alkanethiols need 2–12 hrs compared with short chain alkanethiols or thiols with certain end groups different from –CH₃ that need at least 24 h to form a well-ordered SAM.

When using dithiols, the SAM is developed using the following reactions:



Moreover, dithiols provide a more stable SAM compared to alkanethiols because of the formation of two thiolate bonds per molecule in dithiols and their reductive peak potentials are more negative [38, 39]. On the other hand, these bonds can hinder the transition from the lying down to the standing up configuration, particularly in dithiols with short chain length, resulting in smaller chain-chain interactions, smaller gain in energy and thus higher stability.

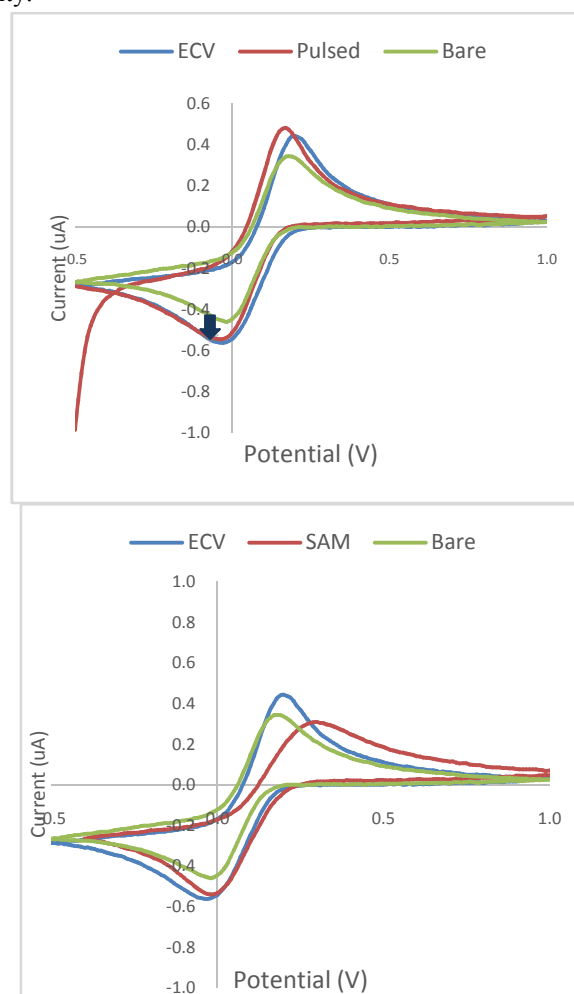


Figure 5. Comparison of voltammograms of bare electrodes and electrodes developed by each of the above-mentioned techniques in 0.1 mM $K_3[Fe(CN)_6]$

Taking this all into account, we decided to use 1, 8-octanedithiol. Figure 5 shows a considerable increase in the electrical response after SAM development. In comparison to LBL, the self-assembly (SA) technique provided a more stable nanoparticle layer (less than 5% variability in peak currents after 10 successive CVs)(Figure 6).

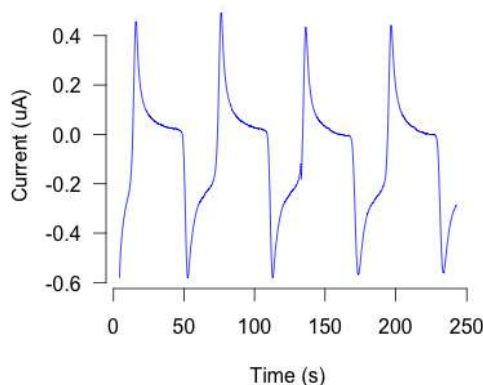
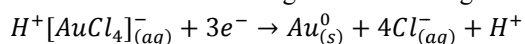


Figure 6. Voltammograms of electrodes prepared using method 2 in 0.1 mM $K_3[Fe(CN)_6]$ over time.

Method 3:

Electrochemical deposition is an important technique as it not only involves simple instrumentation and operation but also is versatile and cost effective. It is generally performed through application of an electrical field to a solution containing the ions of the target material. Electrically-enhanced diffusion of the reactive ions towards the electrode followed by an electron transfer from or to the ion, results in oxidative or reductive deposition of the desired material on the electrode, respectively. Figure 7 shows a voltammogram of an ECV process. The reverse scan of the voltammogram in these experiments exhibits the reduction of Au(III) to Au(0), inducing the deposition of AuNPs onto the electrode surface according to the following reaction.



Different protocols have been proposed for gold electrodeposition on gold electrodes. Using them, various morphologies, including rod-like and dendritic gold nanoparticles, have been obtained in a one-step process [40].

a) Cyclic Voltammetry: There was a broad reduction wave at 0.0 V suggestive of AuNP deposition. As the number of cycles increased, there was a sharp oxidation peak at 1.0V. Throughout the electrodeposition process, the current read at this peak increased during each cycle, which is consistent with thermodynamics that predicts an easier growth of previously formed AuNPs than a nucleation of new AuNPs on the electrode. In addition, the peak area of the reduction of gold oxide suggests that a large amount of gold nanoparticles have been deposited onto the surface of the electrode. After 30 repeated scans, there was no more change in peak height or shape.

b) Pulsed electrodeposition: NP-like gold islands were generated on the electrode; the size and density of the islands increased with increasing number of pulsed electrodeposition cycles.

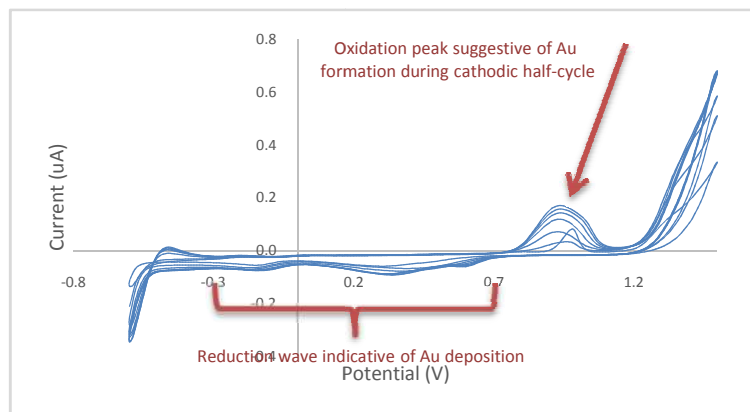


Figure 7. Voltammograms of the ECV process in 1.0 mM $HAuCl_4$ and 0.5 M H_2SO_4 in the presence of 0.1 mM NaCl

Further CV analysis of the electrodeposited electrodes (method 3a) showed higher current compared with methods 1 and 2 (Figure 5), indicating that gold nanoparticles have been successfully attached onto the surface of the electrode and thus improving the conductivity and surface area. The latter is explained later in this article.

The study of the storage stability of the electrodes showed a slight current change (less than 5% variability), showing their long-time stability (Figure 9). This however was not true for the electrodes prepared using pulsed electrodeposition techniques.

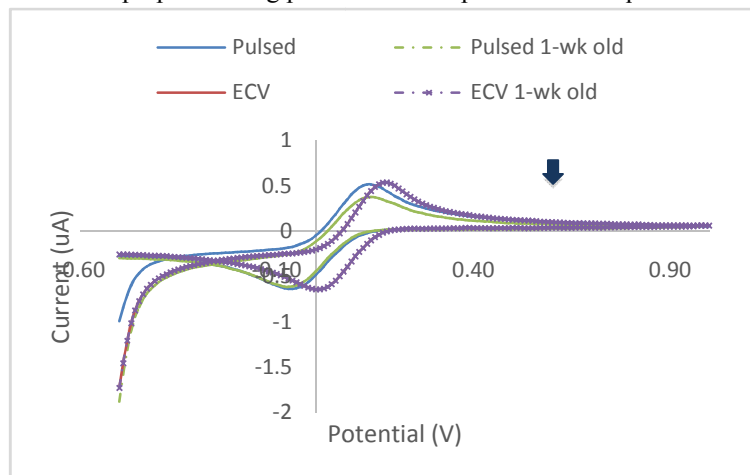


Figure 8. Comparison of voltammograms of electrodes prepared using method 3a and 3b in 0.1 mM $K_3[Fe(CN)_6]$.

The reusability of biosensors is also of great importance. There was no noticeable change of currents during the successive CV cycles (less than 5% variability in peak currents), which implies that the nano-structures, prepared using ECV technique, are firmly immobilized on the gold electrode (Figure 9). Similar to electrodes prepared using SAM techniques, there was no significant current change when assessing the stability of immobilization (less than 5% variability in peak currents measured over time).

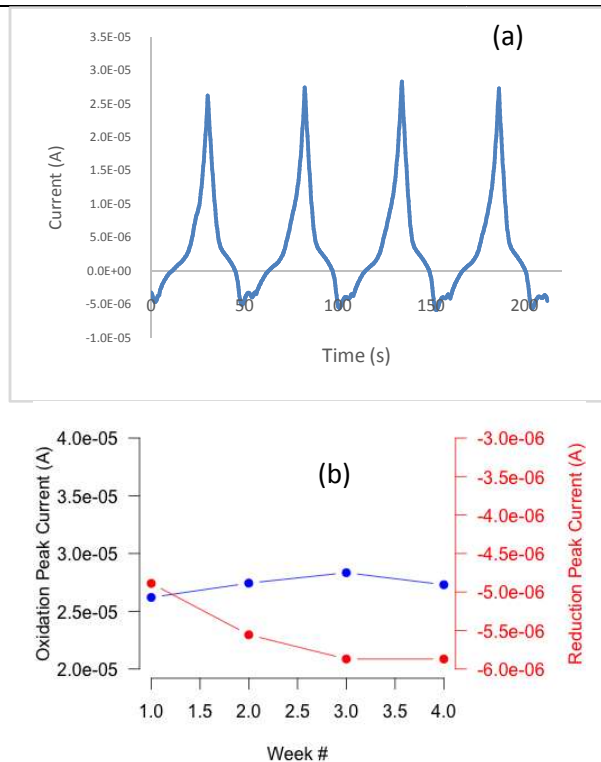


Figure 9. Comparison of voltammograms of electrodes prepared using method 3a in 0.1 mM $K_3[Fe(CN)_6]$ (a) during successive CV cycles (b) over several weeks

The comparison between the different protocols applied in this study is outlined in Table 1. Previous studies have suggested that not only the stability of the AuNP layer but also the density and size of the NPs are of great importance in the sensors' analytical performance, stressing that high density of rather small, spherical-shaped NPs are associated with best responses [41].

Table 1. Pros and Cons of different Au-deposition protocols applied in this study.

		Pros	Cons
1	LBL deposition	Simple and rapid	Unstable, not reproducible
2	SAM development	Strong bonding to underneath layer, stable and reproducible	Time consuming, low sensing performance enhancement
3	Electrodeposition	Acceptable bonding to underneath layer, acceptable sensing performance enhancement, stable and reproducible	Time consuming, No. of cycles depend on the electrode characteristics

Our results suggested that while AuNPs deposited using both SAM and electrodeposition techniques provided a stable layer, the electrodes prepared using electrodeposition showed higher current and thus higher electron transfer rate and analytical performance. This is while many of the previous studies had suggested SAM techniques as an effective way for stable enzyme attachment [42]. It has been evidenced that several factors including the packing density as well as chain length of the SAM play an important role in surface coverage and electron transfer rate. In other words, if the SAM is too densely packed, similar to

our results, it would exhibit a blocking behavior due to its high resistance, a process which would decrease electron transfer rate and subsequently delay the sensing process [43].

Considering the results, the electrodeposition process of AuNP on gold electrode using ECV method was optimized and the focus of the remaining part of this article will be on the characterization of the electrodes modified using this technique.

3.2. Electrochemical characterization.

In this work, AuNPs have been electrodeposited by ECV starting from $HAuCl_4$ (Method 3a). The successful AuNP formation on the treated electrodes was confirmed by showing a typical CV of gold over the potential range of -0.5 V to +1.2 V in 0.5M H_2SO_4 solution (Fig 7b). This voltammogram shows a single sharp reduction peak at +0.2V and oxidation peak at +1.2V.

The increased current noted in further voltammograms confirmed that gold nanoparticles immobilized at the gold interface using this method increased the electrode surface area and facilitate the charge transfer between the AuNPs and the gold electrode (Figure 5).

From the voltammetric responses obtained in $FeCN_6$ information regarding the real electrode surface area and its roughness were extrapolated [44]. The diffusion coefficient of the mediator was calculated by performing CV with three different scan rates (0.1, 0.3, 0.5 V/s). The resulting currents were then plotted against the square root of the scan rate and the obtained slope was equal to the diffusion coefficient. In our case, the diffusion coefficient was calculated to be $5E-08$ cm^2/s .

Chronocoulometry was then performed to measure the electrical charge passing through the electrode as a function of time. The analysis of the chronocoulometric data was then performed based on the Anson equation:

$$Q = 2nFACD^{\frac{1}{2}}\pi^{-\frac{1}{2}}t^{\frac{1}{2}}$$

Herein, Q represents the charge (coulombs), n the number of electrons transferred, A the real electrochemical surface area of the electrode (cm^2), F the Faraday's constant (96,485 coulombs/mol), C the concentration of the mediator (mol/cm^3), D the diffusion coefficient of the mediator (cm^2/s) and t time (s).

The slope of the as expected linear plot between Q and square root of time (a) was used to calculate the real electrochemical surface area of the electrode.

$$A = a/(2nFCD^{\frac{1}{2}}\pi^{-\frac{1}{2}})$$

As expected the real electrochemical surface area of the gold electrodes were calculated to be 0.0784 cm^2 , which is 2.3 times greater than the area before electrodeposition (geometrical area= 0.0225 cm^2). Based on these results, the roughness factor (ratio of electrochemical surface to geometrical surface) was calculated to be 3.49 (compared to 1.53 in bare sputter deposited Au electrodes before electrodeposition). These results were further confirmed with SEM and AFM.

3.3. Density and size characterization.

In order to further characterize the morphology of the nanostructured gold film deposits, SEM (Figure 9) and AFM (Figure 10) analysis was performed. As it was shown earlier, the roughness of the surface increased considerably after

electrodeposition and increasing the number of electrodeposition cycles was associated with growing density of deposited nanoparticles.

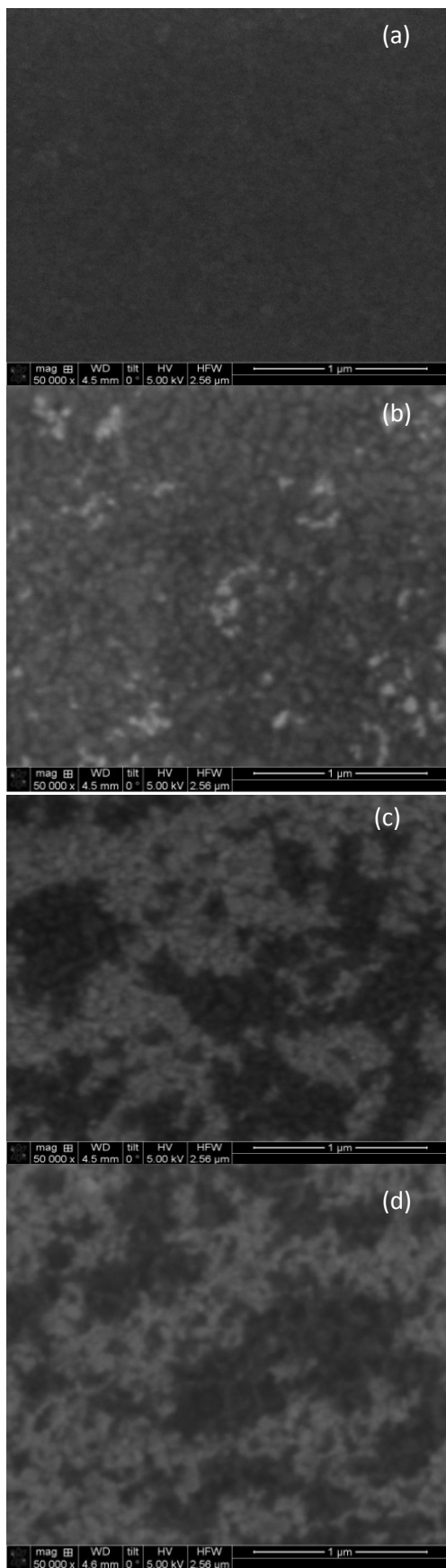


Figure 9. SEM micrographs of a bare gold electrode (a), and gold electrodes after ECV electrodeposition with 5 cycles (b), 10 cycles (c) and 30 cycles (d).

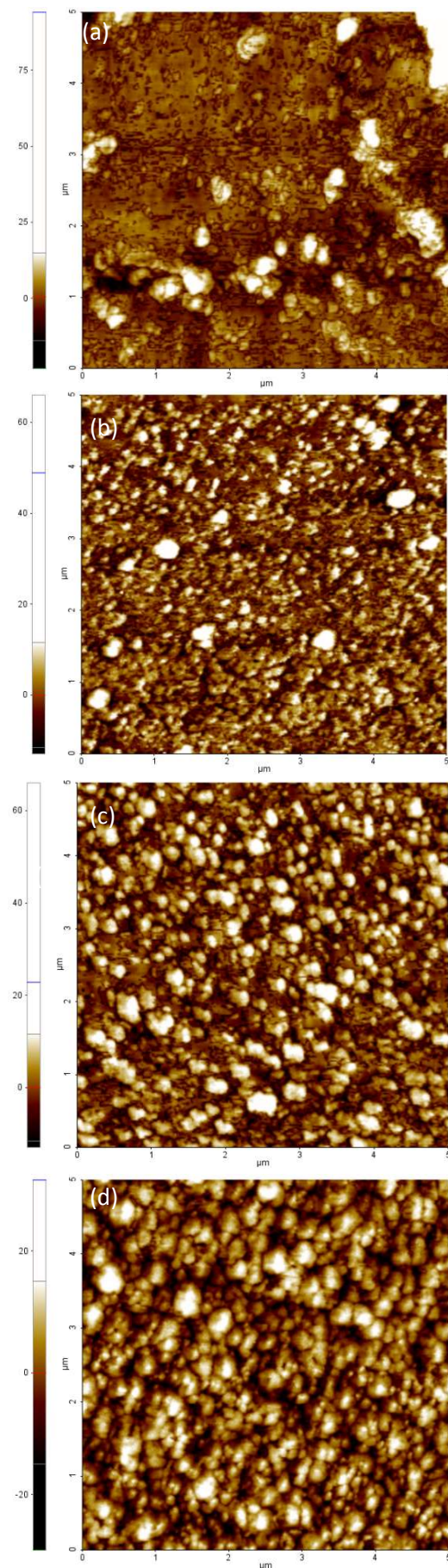


Figure 10. AFM topography of a bare gold electrode (a), and gold electrodes after ECV electrodeposition with 5 cycles (b), 10 cycles (c) and 30 cycles (d); 5*5 μm scan size, set point 11 nm.

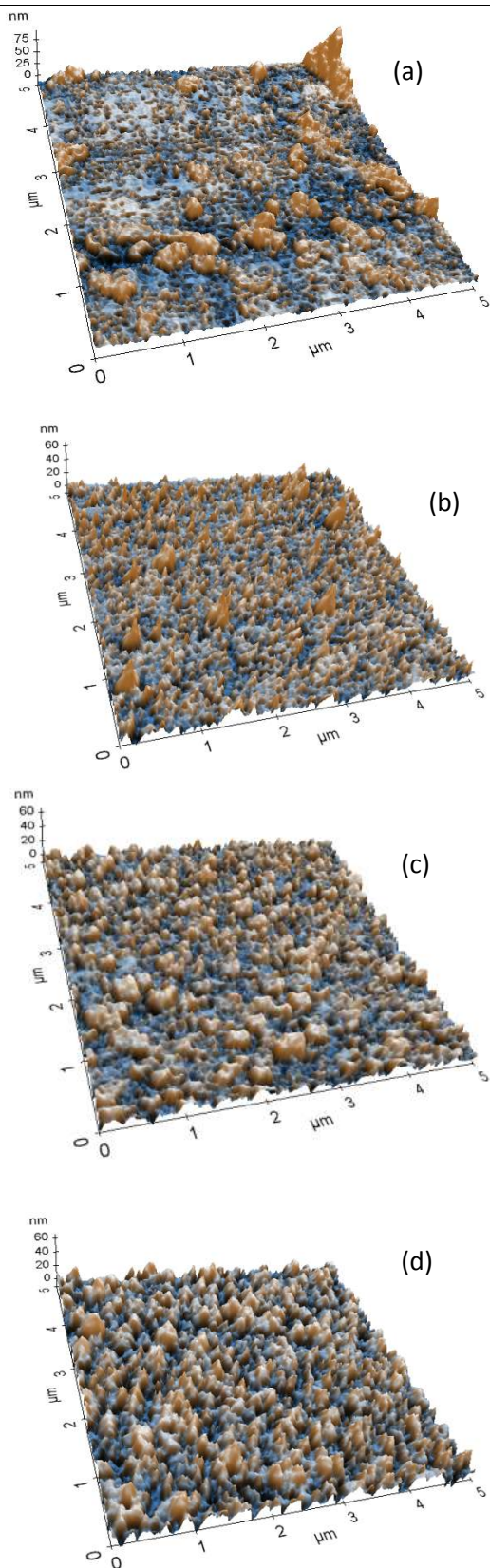


Figure 11. AFM height images of the surface of a bare gold electrode (a), and gold electrodes after ECV electrodeposition with 5 cycles (b), 10 cycles (c) and 30 cycles (d); 5*5 μm scan size, set point 11 nm

Figure 11 shows typical nanopyramidal structures obtained for different electrodeposition conditions. An increased number of deposition cycles were associated with a significant rise in the density of these nanostructures.

STEM images revealed the formation of nanoclusters of gold nanoparticles with the mean size of 20 nm after the ECV process (Figure 12). This is while the electrochemical characteristics of AuNPs are reported to be strongly size-dependent, with 20 nm AuNPs having the most appropriate electrochemical response [45]. The quantum effects, originated by d-band electrons of the surface shifted towards the Fermi-level, enables AuNPs to interact in electrocatalytic reactions.

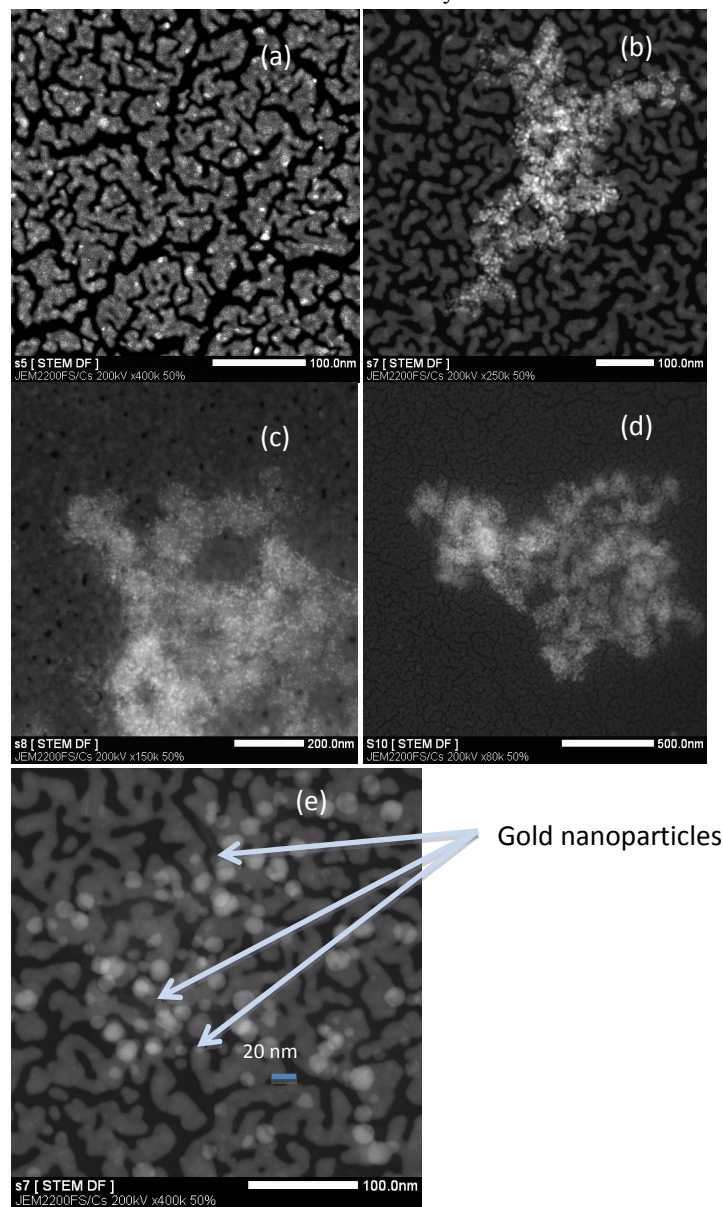


Figure 12. STEM results micrographs of a) bare Au TEM grid before ECV electrodeposition by HAADF contrast, and gold electrodes after ECV electrodeposition with 5 cycles (b), 10 cycles (c) and 30 cycles (d) mean size of the produced nanoparticles (e) by HAADF contrast.

3.4. Stability and Reproducibility.

In order to measure the reproducibility of the as-prepared electrodes, repeatability studies were performed. In this regard peak current in similar CVs performed on a group of electrodes were compared (Figure 13). According to the results, the calculated relative standard deviation was 0.189 (Coefficient of variation= 5.3%), suggesting high likelihood of producing similar electrodes.

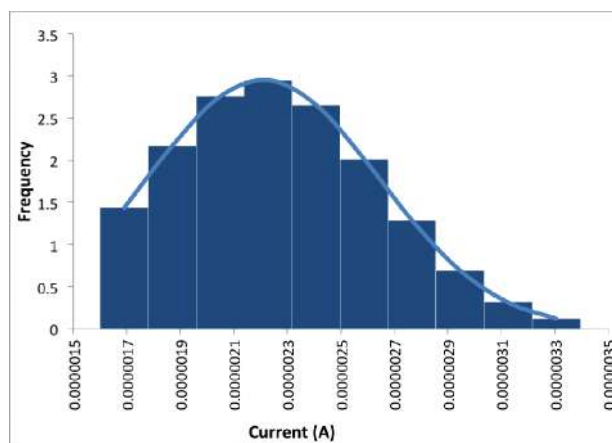


Figure 13. Peak current changes in a group of electrodes prepared using ECV technique.

4. CONCLUSIONS

The deposition of gold nanoparticles (AuNP) on the surface of gold electrodes with the aim of improving its sensing performance is generally conducted in different ways. In this study, the LBL deposition, SAM technique and electrodeposition method were investigated.

The electrode modified through LBL deposition was unstable and not reproducible. Using SAM and ECV techniques on the other hand, the nanostructures were firmly immobilized on the gold electrode prepared, resulting in an acceptable stability and reproducibility. CV-electrodeposition of AuNP (ECV) causes an observable increase in the peak current of recorded CV curves compared to bare Au electrodes, causing improved electrode

kinetics and a reduction in the oxidation potential (thermodynamically feasible reaction). This is attributed to the larger surface area of the modified electrodes and synergistic effects of electrical conductivity and electro-activity of AuNP.

Moreover, electrodes modified using ECV showed better electron transfer rate compared to other studied methods, making them a better candidate for electrochemical sensing purposes. In summary, compared with other discussed methods, gold electrodes from which the surface was modified with gold nanoparticles using ECV presented several advantages with respect to stability, reproducibility and electron transfer rate.

5. REFERENCES

- [1] Daniel M.C., Astruc D., Gold nanoparticles: assembly, supramolecular chemistry, quantum-size-related properties, and applications toward biology, catalysis, and nanotechnology, *Chem. Rev.*, 104, 293-346, **2004**.
- [2] Sreeprasad T., Pradeep T., Noble Metal Nanoparticles. In: Vajtai R, editor. Springer Handbook of Nanomaterials: Springer Berlin Heidelberg, 303-88, **2013**.
- [3] Svarc-Gajic J., Stojanovic Z., Suturovic Z., Marjanovic N., Kravic S., Direct mercury determination in natural waters by chronopotentiometric stripping analysis in macroelectrode process vessel, *Desalination*, 249, 253-9, **2009**.
- [4] Hezarda T., Fajerwerge K., Evrardc D., Collièree V., Behraa P., Grosch P., Influence of the gold nanoparticles electrodeposition method on Hg(II) trace electrochemical detection., *Electrochimica Acta*, 73, 15–22, **2012**.
- [5] Vastarella W., Della Seta L., Masci A., Maly J., De Leo M., Maria Moretto L., PillotonR., Biosensors based on gold nanoelectrode ensembles and screen printed electrodes, *International Journal of Environmental and Analytical Chemistry*, 87, 701-714, **2007**.
- [6] Lia Y., Schluesenerb H.J., Xua S., Gold nanoparticle-based biosensors, *Gold Bulletin*, 43, 29-41, **2010**.
- [7] Jiang C., Markutsya S., Pikus Y., Tsukruk V.V., Freely suspended nanocomposite membranes as highly sensitive sensors, *Nat. Mater*, 3, 721-728, **2004**.
- [8] Kohl P.A., Electrodeposition of Gold, in *Modern Electroplating*, Fifth Edition (eds M. Schlesinger and M. Paunovic), **2010**.
- [9] Etesami M., Mohamed N., Catalytic Application of Gold Nanoparticles electrodeposited by Fast Scan Cyclic Voltammetry to Glycerol Electrooxidation in Alkaline Electrolyte, *Int. J. Electrochem. Sci.*, 6, 4676 – 4689, **2011**.
- [10] Ling T.L., Ahmad M., Heng L.Y., Seng T.C., The Effect of Multilayer Gold Nanoparticles on the Electrochemical Response of Ammonium Ion Biosensor Based on Alanine Dehydrogenase Enzyme, *Journal of Sensors*, **2011**.
- [11] van der Zande B.M.I., Böhmer M.R., Fokkink L.G.J., Schönenberger C., Aqueous Gold Sols of Rod-Shaped Particles, *Phys Chem B*, 101, 852-4, **1997**.
- [12] Green T.A., Gold Electrodeposition for Microelectronic, Optoelectronic and Microsystem Applications, *Gold Bulletin*, 40, 105-114, **2007**.
- [13] Mena M.L., Sedeno P.Y., Pingarron J.M., A comparison of different strategies for the construction of amperometric enzyme biosensors using gold nanoparticle-modified electrodes, *Analytical Biochemistry*, 336, 20–27, **2005**.
- [14] Frens G., Controlled nucleation for the regulation of the particle size in monodisperse gold suspensions, *Nature Phys. Sci.*, 241, 20–22, **1973**.
- [15] Sun X., Dong S., Wang E., One-step synthesis and characterization of polyelectrolyte-protected gold nanoparticles through a thermal process, *Polymer*, 45, 2181–2184, **2004**.
- [16] Basu S., Ghosh S.K., Kundu S., Panigrahi S., Praharaaj S., Pande S., Biomolecule induced nanoparticle aggregation: Effect of particle size on interparticle coupling, *Journal of Colloid and Interface Science*, 313, 724–734, **2007**.
- [17] Noh M.F.M., Tothill I.E., Development and characterization of disposable gold electrodes, and their use for lead(II) analysis, *Anal. Bioanal. Chem.*, 386, 2095, **2007**.
- [18] Wurster E.C., Elbakry A., Göpferich A., Breunig M., Layer-by-Layer Assembled Gold Nanoparticles for the Delivery of Nucleic Acids, *Nanotechnology for Nucleic Acid Delivery Methods in Molecular Biology*, 948, 171-182, **2013**.
- [19] Xue Y., Zhao H., Wu Z., Li X., He Y., Yuan Z., The comparison of different gold nanoparticles/graphene nanosheets hybrid nanocomposites in electrochemical performance and the construction of a sensitive uric acid electrochemical sensor with novel hybrid nanocomposites, *Biosens Bioelectron*, 29, 102-8, **2011**.
- [20] Ottakam Thotiyl M.M., Basit H., Sánchez J.A., Goyer C., Coche-Guerente L., Dumy P., Multilayer assemblies of polyelectrolyte-gold

nanoparticles for the electrocatalytic oxidation and detection of arsenic(III), *J Colloid Interface Sci.*, 383, 130-9, **2012**.

[21] Mani V., Chikkaveeraiah B.V., Patel V., Gutkind J.S., Rusling J.F., Ultrasensitive Immunosensor for Cancer Biomarker Proteins using Gold Nanoparticle Film Electrodes and Multienzyme-Particle Amplification, *ACS nano*, 3, 585-594, **2009**.

[22] Chen H.J., Wang Y.L., Wang Y.Z., Dong S.Z., Wang E.K., One-step preparation and characterization of PDDA-protected gold nanoparticles, *Polymer*, 47, 763-766, **2006**.

[23] Ron H., Matlis S., Rubinstein I., Self-Assembled Monolayers on Oxidized Metals. 2. Gold Surface Oxidative Pretreatment, Monolayer Properties, and Depression Formation, *Langmuir*, 14, 1116-1121, **1998**.

[24] Tang Y.Y., Chen P.Y., Gold Nanoparticle-electrodeposited Electrodes Used for p-Nitrophenol Detection in Acidic Media: Effect of Electrodeposition Parameters on Particle Density, Size Distribution, and Electrode Performance, *Journal of the Chinese Chemical Society*, 58, 723-731, **2011**.

[25] Takahashi Y., Umino H., Taura S., Yamada S., An Electrochemical Approach for Fabricating Organic Thin Film Photoelectrodes Consisting of Gold Nanoparticles and Polythiophene, *Rapid communication in photoscience*, 2, 79-81, **2013**.

[26] Pingarron J.M., Yanez-Sedeno P., Gonzalez-Cortes A., Gold nanoparticle-based electrochemical biosensors, *Electrochimica Acta*, 53, 5848-5866, **2008**.

[27] Finot M.O., Braybrook G.D., McDermott M.T., Characterization of electrochemically deposited gold nanocrystals on glassy carbon electrodes, *Journal of Electroanalytical Chemistry*, 466, 234-241, **1999**.

[28] Penga H.P., Hua Y., Liua A.L., Chena W., Lina X.H., Yub X.B., Label-free electrochemical immunosensor based on multi-functional gold nanoparticles-polydopamine-thionine-graphene oxide nanocomposites film for determination of alpha-fetoprotein, *Journal of Electroanalytical Chemistry*, 712, 89-95, **2014**.

[29] Backman M., Juslin N., Nordlund K., Bond order potential for gold, *The European Physical Journal B*, 85, 317, **2012**.

[30] Kaulen C., Homberger M., Bourone S., Babajani N., Karthäuser S., Besmehn A., Simon U., Differential Adsorption of Gold Nanoparticles to Gold/Palladium and Platinum Surfaces, *Langmuir*, 30, 574-583, **2014**.

[31] Verma H.N., Singh P., Chavan R.M., Gold nanoparticle: synthesis and characterization, *Veterinary World*, 7, 72-77, **2014**.

[32] Hu M., Chen J., Li Z.Y., Gold nanostructures: engineering their plasmonic properties for biomedical applications, *Chem Soc Rev*, 35, 1084-94, **2006**.

[33] Chen H., Zhao G., Construction of Ionic Liquid Self-assembled Monolayer on Gold Electrode for Hemoglobin Modifying and Peroxide Biosensing, *Int. J. Electrochem. Sci.*, 7, 12907 - 12921, **2012**.

[34] Łuczak T., Gold and Nanogold Electrodes Modified with Gold Nanoparticles and meso-2,3-Dimercaptosuccinic Acid for the Simultaneous, Sensitive and Selective determination of Dopamine and Its Biogenic Interferents, *Electroanalysis*, 26, 2152-2160, **2014**.

[35] Łuczak T., Comparison of electrochemical oxidation of epinephrine in the presence of interfering ascorbic and uric acids on gold electrodes modified with S-functionalized compounds and gold nanoparticles, *Electrochim Acta*, 54, 5863-5870, **2009**.

[36] Vericat C., Vela M.E., Benitez G., Carrob P., Salvarezza R.C., Self-assembled monolayers of thiols and dithiols on gold: new challenges for a well-known system, *Chem. Soc. Rev.*, 39, 1805-1834, **2010**.

[37] Daza Millone M.A., Hamoudi H., Rodríguez L., Rubert A., Benítez G.A., Vela M.E., Self-Assembly of Alkanedithiols on Au(111) from Solution: Effect of Chain Length and Self-Assembly Conditions, *Langmuir*, 25, 12945-12953, **2009**.

[38] Tour J.M., Jones II L.R., Pearson D.L., Self-assembled monolayers and multilayers of conjugated thiols, α , ω -dithiols and thioacetyl-containing adsorbates. Understanding attachments between potential molecular wires and gold surfaces, *J American Chemistry Society*, 117, 9529, **1996**.

[39] Ling T.L., Ahmad M., Heng L.Y., Seng T.C., The Effect of Multilayer Gold Nanoparticles on the Electrochemical Response of Ammonium Ion Biosensor Based on Alanine Dehydrogenase Enzyme, *J of Sensors*, **2011**.

[40] Tian Y., Liu H., Zhao G., Tatsuma T., Shape-Controlled Electrodeposition of Gold Nanostructures, *J. Phys. Chem. B*, 110, 23478-23481, **2006**.

[41] Wu J., Li L., Shen B., Polythymine Oligonucleotide-Modified Gold Electrode for Voltammetric Determination of Mercury(II) in Aqueous Solution, *Electroanalysis*, 22, 479-482, **2010**.

[42] Park B.W., Kim D.S., Yoon D.Y., Surface modification of gold electrode with gold nanoparticles and mixed self-assembled monolayers for enzyme biosensors, *Korean J Chem Eng*, 28, 64-70, **2011**.

[43] AlShamaileh E., Saadeh H., Favry V., Modification of gold Surface with gold nanoparticles and Cyclohexyl Dithiocarbamate as a Selective Sensor for Cysteine, *Journal of Chemistry*, **2013**.

[44] Fragkou V., Ge Y., Steiner G., Freeman D., Bartetzko N., Turner A.P.F., Determination of the real surface area of a screen-printed electrode by chronocoulometry, *Int J Electrochem Sci*, 7, 6214-20, **2012**.

[45] de La Escosura-Muñiz A., Parolo C., Maran F., Mekoçi A., Size-dependent direct electrochemical detection of gold nanoparticles: application in magnetoimmunoassays, *Nanoscale*, 3, 3350-3356, **2011**.